IEEE Access
Multidisciplinary | Rapid Review | Open Access Journal

Received July 16, 2019, accepted August 23, 2019, date of publication September 11, 2019, date of current version October 2, 2019.

Digital Object Identifier 10.1109/ACCESS.2019.2940894

Line Impedance Measurement to Improve Power Systems Protection of the Gautrain 25 kV Autotransformer Traction Power Supply System

NDAEDZO M. MOYO[1,2], RAMESH C. BANSAL[3], (Senior Member, IEEE), RAJ NAIDOO[2], (Senior Member, IEEE), AND WILLEM SPRONG[4]

[1]Bombela Maintenance (Pty) Ltd., Gautrain Maintenance Depot, Midrand 1684, South Africa
[2]Department of Electrical, Electronic and Computer Engineering, University of Pretoria, Pretoria 0002, South Africa
[3]Department of Electrical and Computer Engineering, University of Sharjah, Sharjah, United Arab Emirates
[4]GIBB, Johannesburg 2191, South Africa

Corresponding author: Ndaedzo M. Moyo (ndaedzo.moyo@bombardiersa.co.za)

This work was supported by the Electrical, Electronic and Computer Engineering Department, University of Pretoria.

ABSTRACT Traction power systems are susceptible to service affecting electrical faults or disturbances. These may cause interruptions of the power supply to the trains, affecting systems operations and causing major delays. Therefore, accuracy in fault reporting and fault location is vital in the decision-making processes that will result in shorter outage periods.The evaluation and analysis of traction power protection systems has become vital to improve the system reliability and reduce outages and related costs. Line impedance measurements form an integral part of fault analysis and distance location due to the use of impedance relays in protection systems. This paper shows the importance of conducting impedance measurements in order to improve the accuracy of distance protection relays. In this paper, impedance measurements were conducted and the measured results were compared with the theoretical values. The feeder to earth, catenary to earth and feeder to catenary impedance measurements were conducted and used in the impedance calculations and analysis. The earth resistances for all line sections were also measured. Furthermore, the line impedance measurements were used for the calculation of the compensation for the earth return factor with specific application in protection settings optimisation for a traction power system. This has helped to improve the accuracy of the protection parameters. The protection settings parameters were revised as a result.

INDEX TERMS Impedance measurements, power system, protection, feeder, catenary, traction, autotransformer.

I. INTRODUCTION

Ever since the Gautrain project in Johannesburg, South Africa, was commissioned in June 2010, a lot of power system faults have been experienced and efforts have been made to adjust the relay parameters in order to improve the protection system. Line impedance measurements were taken as part of improving the protection settings accuracy. For a distance protection relay to detect and operate for a fault accurately, the relay depends on the accuracy of the impedance settings. Fault-loop impedance measurements form an integral part of distance protection relays [1].

The measurement of line impedance as it applies to power transmission lines has been studied before [2]–[4], but in this paper, the measurement of impedances and the application of the results and its benefits is applied to an existing autotransformer traction system. The concept of distance protection for traction overhead wiring (OHW) is the same as that of power system transmission lines, however, the configuration of the protected system is different and the load is dynamic. The contribution of voltage and current of this dynamic load is discussed in section II. The existence of rail, the aerial earth conductor (AEC) and the buried earth conductor (BEC) impedances, as well as the configuration of the catenary conductors and feeder conductors, makes it different from that of transmission lines.

The combination of the catenary wire and the contact wire is generally known as the ''catenary system''. This consists of a catenary wire and a contact wire which is supported by droppers throughout the alignment. The catenary wire

The associate editor coordinating the review of this manuscript and approving it for publication was Padmanabh Thakur.

has different properties and impedance from the contact wire but the two are designed to share the current. In addition, the entire OHW network has several tensioning weights and overlaps which also contribute to the difference in impedance when compared to transmission lines. Overlaps are when two catenary wires, connected in the middle by a jumper, run in parallel for about two to three spans at the beginning/end of tension lengths. Each end is connected to a tensioning weight whose prime purpose is to restrict the sag and elongation due to temperature variations. This arrangement of the catenary system as described in this paragraph makes it complicated to obtain correct impedances from the conductor specifications and apply them as a function of distance without conducting measurements, as is often the case with power transmission lines.

In a distance protection scheme such as the one discussed in this paper, two similar relays are installed at substations on both ends of the line. Both these relays detect the fault and send communications signals to each other so as to isolate and eliminate the fault. The accuracy of the impedance values plays a major role in this activity. Distance protection systems require correct system parameters and accurate relay settings to improve the accuracy of the protection system [2], [4]. The earth conditions can influence voltage and current values [3], [5], hence, there is need for on-site measurements which would give relatively accurate parameters.

In this paper, a multi conductor power transmission line approach to determine the self and mutual impedances is undertaken [2], [6]. The difference in the theoretical, calculated impedances from the conductor supplier and the physically measured values; and its application in impedance protection settings is analysed and discussed. The other benefit of conducting line impedance measurements is the ability to use the results for the calculation of the compensation for the earth return factor for protection settings optimisation. This factor has been identified as a contributing factor to the accuracy of the impedance settings [4]. References [2]–[4] have done research on this factor with reference to high voltage (HV) transmission lines, however, further application in relation to 2 × 25 kV AC traction systems has not been encountered during this research. In the Gautrain, this factor has been set to a default value or factory recommended setting. In this paper, the measured impedances are used to calculate the compensation for the earth return and its correct usage in relation to 2 × 25 kV AC traction systems is further discussed.

The Gautrain is a rapid rail system that transports passengers between Pretoria and Johannesburg, and between Johannesburg and OR Tambo International Airport in South Africa. The Gautrain power supply system consists of one Main Propulsion Substation (MPS) and five remotely located autotransformer paralleling substations (APSs). The electric traction system typically receives high voltage (HV) power at the MPS from a high voltage primary source and steps it down to lower voltages for distribution to trains. In the South African context, its uniqueness in being the only rapid rail system with train design speeds of 160 km/h and its employment of the APSs makes it interesting in conducting research on system performance related subject matters.

Each traction power system around the world has its own challenges in terms of performance and power system protection because each one has different design parameters, unique earth and environmental considerations, different impedances, unique train/overhead wiring (OHW) interaction and different protection philosophies. Contrary to the Gautrain, some traction systems in other research have two traction supply stations at both ends of the track with several APS along the way [7], hence, the need to study Gautrain as a different system from other systems around the world. The series impedances of the traction transformers and the autotransformers are of important consideration [8], although this paper only discusses the line impedances of the OHW equipment between the substations.

This paper is organised as follows: section I is the introduction, section II describes the Gautrain power supply system, section III describes the APS, and section IV describes distance protection and line impedance in traction systems. Section V gives an analysis of the line impedances of the Gautrain 25 kV AC traction system, section VI explains the OHW line impedance measurements set-up, section VII are the results, section VIII are the discussions and analysis of results, and section IX is the conclusion.

II. GAUTRAIN POWER SUPPLY SYSTEM

The Gautrain System receives 88 kV AC, 50 Hz from the national power supply company Eskom and steps it down to 50 kV (2 × 25 kV) AC using 4 × 40 MVA traction transformers. The 88 kV AC power is supplied from a three-phase network and only two phases per transformer are connected as shown in Figure 1. For security of high voltage primary power supply, redundancy is provided by supplying from two different Eskom feeders with enough capacity to supply the entire Gautrain network per Eskom feeder. The Eskom feeders are connected at two different substations that also have different power supply sources.

Figure 1 is a simplified circuit of the Gautrain power supply and distribution (PS&D) system. The diagram shows the

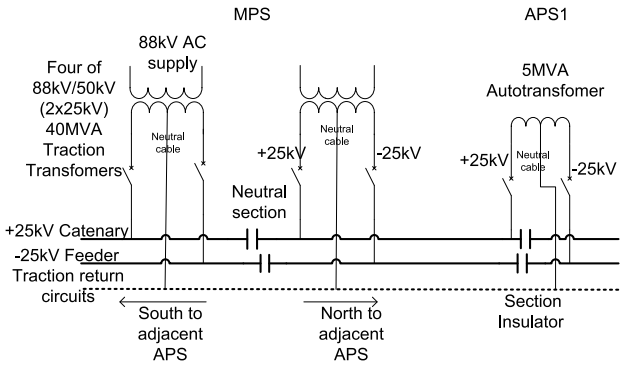

FIGURE 1. Simplified gautrain power supply and distribution system showing two out of four 40 MVA transformers and one of five APSs.

configuration of the 88 kV: 50 kV (2 × 25kV) transformers and how they are connected to feed the track to the south and to the north of the MPS. Outside the MPS on the OHW there is a neutral section to separate the different phases when the trains move from the north to south of the MPS and vice versa. This is also known as a phase split in other systems [9].

Figure 1 shows how the catenary and the feeder are connected to the OHW and how the neutral of the traction transformers and the autotransformer are connected to the traction return circuits. For simplicity, one APS with a 5 MVA, 25 kV AC autotransformer is shown out of a total of five APS comprising of two APSs in the south and three APSs in the north with the smallest APS having one autotransformer and the biggest with three autotransformers.

The functioning of all the APSs is the same but its sizing and location relative to the MPS and relative to each other is based on power flow and load flow calculations and simulations. In this case the shortest distance between the substations is 5.14 km and the furthest is 17.98 km.

In the MPS, two of the four transformers supply the north of the lines towards Pretoria and the other two supply the south towards Park station in Johannesburg and OR Tambo airport. In each direction only one of the transformers is used at any given time with the other transformer being used for back up. This arrangement forms an n-1 redundancy in each direction north and south of the MPS in case one of the transformers fails or needs to be switched off for maintenance. The arrangement further gives more flexibility for the entire network to be supplied using only one transformer with a reduced load and with the neutral section closed. The two Eskom HV feeders are separated by a bus-section which gives the flexibility to supply the entire system from either of the HV feeders by closing the bus-section. The neutral terminal on the secondary side of each MPS transformer is connected to a common neutral busbar, which in turn is earthed to the MPS ground/earth grid and connected to the rail and aerial earth conductors of the OHW. Similarly, at the APS, the neutral terminals of the autotransformers are also connected to a common neutral busbar, which is also connected to the earth grid, the rail and the aerial earth conductors of the OHW.

Figure 2 shows the OHW arrangement. The 25 kV AC is distributed to the OHW in the form of two conductors (2 × 25 kV) for use by the trains. The OHW consists of catenary/contact conductors, feeder conductors and the earth wire. The return circuit consists of the rail tracks, the AEC and the BEC which is installed along the entire track. The return circuit is also connected to the earth grids of the MPS and the APSs as well as the neutral busbars in all the substations. Power is continuously transferred to the trains through the train pantograph which collects power from the contact wire at 25 kV AC.

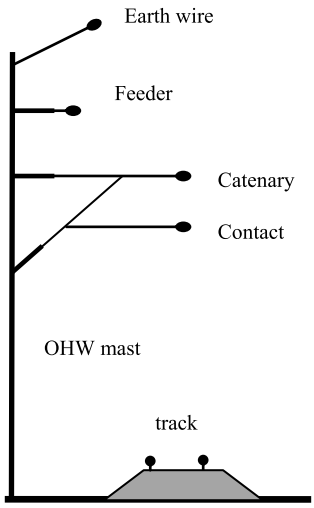

FIGURE 2. OHW arrangement.

TABLE 1. Voltage of overhead contact line [10].

Classification	Voltage
Highest Non-permanent Voltage	29 kV
Highest Permanent Voltage	27.5 kV
Nominal Voltage	25 kV
Lowest Permanent Voltage	19 kV
Lowest Non-permanent voltage	17.5 kV

III. AUTO-TRANSFORMER PARALLELING SYSTEMS

As can be expected, there are severe voltage drops along the OHW power distribution system, hence, the APSs are located at remotely distributed points in the system as per design calculations and load flow studies [5]. The APSs are designed to keep voltages in admissible ranges that are given in Table 1 [10]. At the APS, the voltages are balanced between the catenary and the autotransformer neutral, and between the feeder and the autotransformer neutral, and the return current is distributed in a balanced manner between the two phases [8]. In this configuration, there is a 180° phase difference between the feeder and the catenary [8], [11]. The catenary wire is considered to be positive and the feeder wire is negative [7]. In the APS configuration, the return current flows in the AEC, rail and the BEC.

As compared with other AC traction power supply systems such as the booster transformer system, the autotransformer is found to be the most suitable for this application. Its advantage is that it can be implemented with a smaller number of substations and that the use of higher voltages makes it more efficient as this results in lower losses [5], [9]. The autotransformer traction supply system has lower currents, voltage drop, and electromagnetic interference with the communication lines [12]. The distance between APSs is long, up to 15-18 km as compared to booster stations which are 3 to 5 km apart [11]. The voltage level of the system is considered to be double as it is 50 kV AC between the catenary and the feeder [11], hence lower losses for the same power drawn from the system as compared to booster systems in addition to lower voltage drops [11], [13]. Autotransformers are always energised whereas booster transformers get energised only

when there is a train in the vicinity [11], [13]. A booster transformer forces the current through the catenary and the return circuit to be equal. This configuration minimises the leakage current through the ground [11]. It is also advantageous that the HV source of the 88 kV AC supply is at one location rather than in many locations along the system as the APS does not require any HV supply. Any variations in voltages are regulated using the tap changers that form part of the MPS traction transformers. Electromagnetic interference (EMI) problems between the traction and the other circuits such as communication and signalling are eliminated by the design [5], [9], [12]. The APS configuration for a complete APS with two autotransformers is shown in Figure 3.

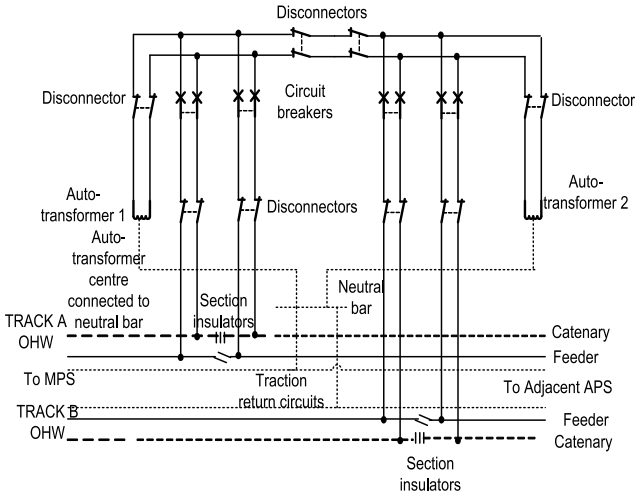

FIGURE 3. APS configuration circuit.

An explanation of how the APS system works is best illustrated in the current distribution diagram in Figure 4[12], [13]. In Figure 4, the autotransformer substation is under load if there are trains in proximity or in sections supplied by that substation [13], [14]. The current in the traction return circuit (I) is equal to the total current in the autotransformer (I/2+I/2) as shown in Figure 4 [15]–[17].

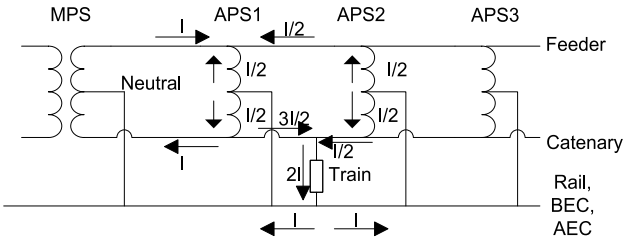

FIGURE 4. Current distribution in an autotransformer system.

The autotransformer primary side is connected from the OHW between the feeder and catenary, and the secondary is the centre tap connection between the feeder and the catenary. This kind of configuration is also found in other autotransformer traction systems around the world [14], [15], [17].

The centre tap of each autotransformer is connected to the rails immediately outside the APS enclosure and to the earth wire via overhead cables. Research in [14] also describes a system which is close to the Gautrain system in design except for the supply voltages which are higher. In addition, the rails are connected to the buried earth conductor (BEC) which runs along the entire rail. The autotransformer configuration gives a voltage of 25 kV AC between the catenary and earth, and a voltage of 25 kV AC between feeder and earth. Therefore, the voltage between the feeder and catenary is 50 kV AC.

IV. DISTANCE PROTECTION AND LINE IMPEDANCE IN TRACTION SYSTEMS

Line impedance measurements form an integral part of power systems protection because these systems use what is commonly known as distance protection or impedance protection. Protection for OHW uses distance or impedance protection as discussed in this paper. The impedance relays in their configuration work by measuring the loop impedance using voltage and current signals [1]. A description of how fault loop impedance measurement is conducted for transmission lines is mentioned in [1], [4] and the same principle can be applied to traction systems. This is illustrated in Figure 9. The equivalent model of a traction system can be constructed using equivalent self-impedances and mutual-impedances of the system [18], [19].

In several research papers [20]–[22], it is proposed that the OHW system could be expressed by a reduced equivalent model which represents the feeder, the catenary/contact wire conductor group, and return/grounded circuits. The same approach is used in this paper. The return/grounded circuit consisting of the rail, earth wire and BEC are generally grouped together [9]. This is illustrated and discussed in section V of this paper. The path of the return currents and the faults currents is through the rail and the other conductors that are at earth potential [9].

The following types of faults are found in a traction power supply system such as the Gautrain:

- Catenary-to-ground fault
- Feeder-to-ground fault
- Feeder-catenary-to-ground fault
- Feeder-to-catenary fault (no ground)
- Earth fault
- Overcurrent fault

On adopting the protection relays to traction systems, catenary-to-ground and feeder-to-ground faults are in essence phase-to-ground faults and the catenary-to-feeder faults are phase-to-phase faults. Hence in a 2 × 25 kV the loop impedance, referred to in [2]–[4] for transmission lines will be either between catenary, feeder and earth, or between either feeder and earth or catenary and earth. When these faults occur, both the feeder and catenary circuits are disconnected by means of double pole circuit breakers on both ends of the line section in response to a trip signal or command issued by the distance protection relays [8]. In order

TABLE 2. Zones and operating times.

Zone	Direction	Operating time (s)
Zone 1	Forward	0
Zone 2	Forward	0.4
Zone 3	Non-directional	1.0

to trip selectively, the impedance settings should be correct and like in transmission lines, the protected lines for traction systems are also defined and divided into protection zones as in Zone 1, Zone 2 and Zone 3. The auto-reclose cycle and the lockout procedure of circuit breakers are as defined in protection philosophies of companies designing the protection systems. Protection settings are designed for sensitivity to detect all potential faults, and to clear the faults as fast as possible, selectively clearing only the part of the network that has a power system fault. This improves system reliability because only circuit breakers that are required to operate will open to isolate the fault.

In general, in order to fulfil the distance protection philosophy of a traction power supply system, the relays on both ends of the line are interconnected using fibre optic cables to act as a communication link for the transmission of the permissive trip signals.

In the Gautrain, the relays used have quadrilateral characteristics which have been designed not to encroach the traction load. The zone 1 reach of each relay is set to 85% of the line section impedance between the substations taking into consideration current transformer (CT), voltage transformer (VT) and relay errors. This again illustrates the importance of correct impedance values as this might result in over-reaching if incorrect impedance values are used. The zone 2 reach is set to be more than 100% of the protected section to reach beyond the transformers in the end-of section substation with reference to the relay being set. This is set with a delay time, whereas, zone 1 is set to trip instantaneously with a single attempt auto-reclose (ARC) allowed. Both zone 1 and zone 2 are set to be in the forward direction, whereas zone 3 which acts as a back-up is set to be non-directional with a time delay to cover the entire network. For Zone 3, non-directional means that the settings can either be forward or reverse looking. In this case, the forward direction is set on the feeding substation relays and the reverse is set for the incoming relays. All these settings are subject to the protection philosophy of the utility implementing the settings and may differ from one traction project to another. The summary of the operating times of each zone for the system in this case study is given in Table 2.

V. LINE IMPEDANCE ANALYSIS OF GAUTRAIN 25 kV AC TRACTIONS SYSTEM

In this section, the relationship between the impedances of the return circuit and the OHW circuits is presented. Although the Gautrain railway system consists of two tracks, for analysis, only one of the tracks is used in this paper. Mathematical modelling of 25 kV traction systems involves the interaction of feeder and catenary conductors with ground and earth wires. This modelling is complex as it also involves the magnetic and electric field relationship between different conductors, as well as distributed conductance of the conductors [23]. Research in [23] discusses the power frequency and power quality; hence, these models are discussed in a greater detail, and also include the electromagnetic relationship between the live conductors and the ground conductors as compared to this paper whose main focus is the accuracy of line impedances.

The relationship between the return circuit impedances is shown in Figure 5.

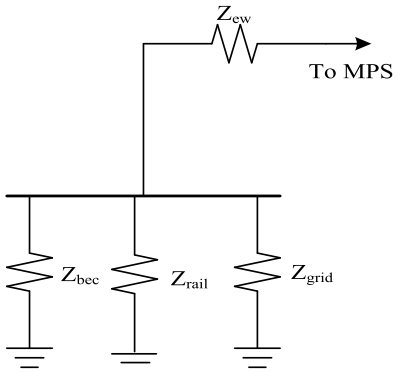

FIGURE 5. Traction return circuit impedances.

This comprises the earth wire impedance Z_{ew}, also known as the aerial earth conductor (AEC), substations earth grid impedance Z_{grid}, the impedance of the buried earth conductor Z_{bec} and the rail impedance Z_{rail}. The value of Z_{ew} is determined by the AC impedance of the aerial earthing conductor and the distance between the APS and the MPS. The values of Z_{bec} and Z_{grid} are determined by the geometry of the buried earthing conductor, the geometry of the earthing grid, conductor-to-earth conductance, rail-to-earth conductance and the soil resistivity in the local area [4], [5], [24].

This interconnection is best illustrated using Figure 6. Figure 6 shows the interconnection between the AEC, BEC, rail and the APS earthing grid. At each APS location there is an earthing grid installed within the perimeter of the APS reserve. All electrical equipment is earthed, and metal support structures within the APS are electrically connected to the earthing grid. The APS earthing grid is electrically connected to the buried earthing conductor and to the aerial earthing conductors.

In the event of a fault within the APS, fault current will be returned to the MPS or dissipated to remote earth via the MPS and APS earthing grids, the buried earthing conductor and the aerial earthing conductors. The amount of current flowing through each return path is dependent on the resistance of the return path.

The impedances of a section of line between the MPS and the APS or between two APSs can be summarized by

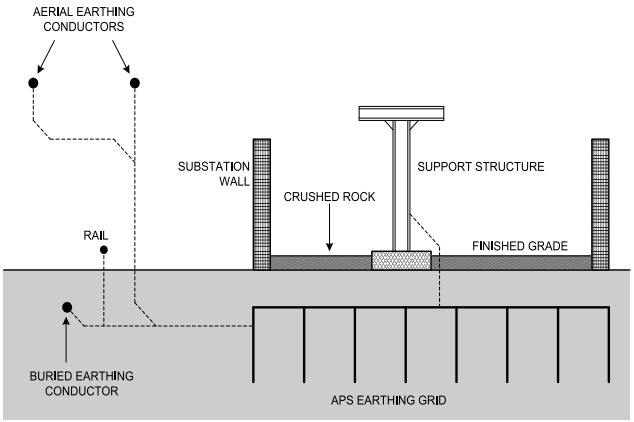

FIGURE 6. Traction return circuit connection at the APS.

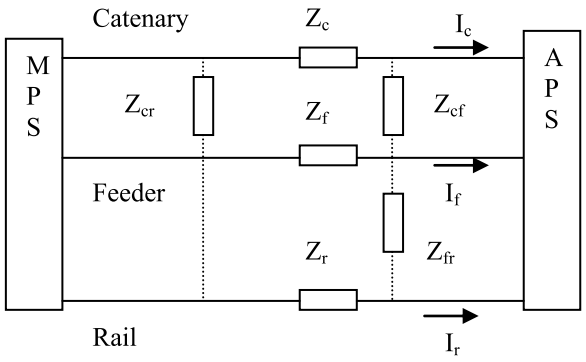

FIGURE 7. Equivalent electric circuit of a section of line.

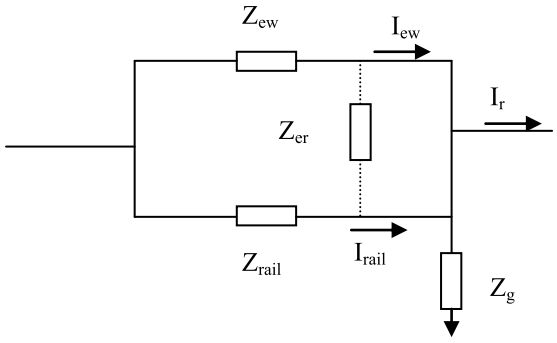

FIGURE 8. The railway equivalent impedance of the grounded circuit.

Figures 7 and 8. Figure 7 and 8 does not take into consideration the impedances of the MPS transformers and the APS autotransformers.

The impedances in Figures 7 and 8 are defined as follows:

Z_{ew}, Z_{bec}, Z_{grid} are the impedances of the aerial earthing conductor which runs on the overhead along the entire railway between the APS and the MPS, the buried earthing conductor to remote earth, and the substation earthing conductor to remote earth respectively.

Z_c is the catenary wire impedance, Z_f is the feeder wire impedance, and Z_r is the railway equivalent impedance of the grounded circuit consisting of Z_{ew} and Z_{rail}. Z_{rail} is the impedance of the rails and the BEC which is buried parallel the rail (in case of the Gautrain), and Z_g is the rail-ground impedance.

The mutual impedances are defined as follows:

Z_{cf} is the mutual impedance of the catenary and the feeder, Z_{cr} is the mutual impedance of the catenary and the grounded circuit, Z_{fr} is the mutual impedance of the feeder and the grounded circuit, and Z_{er} is the mutual impedance of the earth wire and the rail.

The grounded circuit in Figure 5 can be expressed as follows [25], [26]:

$$Z_{ew}I_{ew}+Z_{er}I_{rail}=Z_{rail}I_{rail}+Z_{er}I_{ew}=Z_rI_r \quad (1)$$

$$I_{rail}+I_{ew}=I_r \quad (2)$$

From 1 and 2,

$$I_{rail}=\left(\frac{Z_{ew}-Z_{er}}{Z_{rail}+Z_{ew}-2Z_{er}}\right)I_r \quad (3)$$

and

$$I_{ew}=\left(\frac{Z_{rail}-Z_{er}}{Z_{rail}+Z_{ew}-2Z_{er}}\right)I_r \quad (4)$$

Substituting (3) and (4) into (1) gives the following equation of the equivalent circuit [25]:

$$Z_r=\left(\frac{Z_{ew}Z_{rail}-Z_{er}^2}{Z_{rail}+Z_{ew}-2Z_{er}}\right) \quad (5)$$

The relationship between the mutual impedances of the catenary and rail equivalent impedance in Figures 7 and 8 can be expressed as [25]:

$$Z_{cr}=\left(\frac{Z_{cew}}{Z_{ew}}+\frac{Z_{crail}}{Z_{rail}}\right)Z_r \quad (6)$$

where Z_{cew} is the mutual impedance of the catenary and the earth wire and Z_{crail} is the mutual impedance of the catenary and the rail.

The relationship between the mutual impedances of the feeder and rail equivalent impedance can be expressed as [25], [26]:

$$Z_{fr}=\left(\frac{Z_{few}}{Z_{ew}}+\frac{Z_{frail}}{Z_{rail}}\right)Z_r \quad (7)$$

where Z_{few} is the mutual impedance of the feeder and the earth wire and Z_{frail} is the mutual impedance of the feeder and the rail.

The amount of fault impedance does not affect the line impedance calculations. The line impedance is fixed once a type of conductor and the length of line is determined or in this case once the impedance is measured and included in the calculation and determination of the relay characteristic and settings. The line impedance, therefore, does not change, however the fault impedance itself varies depending on the type and location of the fault. These fault impedances regardless of fault type must be within the characteristics of the relay

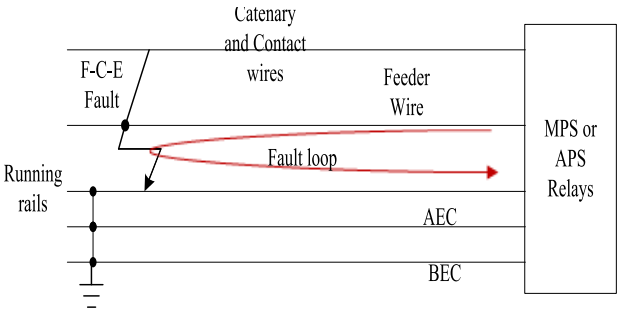

FIGURE 9. Fault loop for a feeder to catenary to earth fault (F-C-E).

in order for it to operate. During a fault condition, the measured fault current increases and the voltage gets depressed, and the impedance as measured by the relays decreases, thereby initiating a trip command. For the impedance protection to work accurately, the line impedances are set as per the line impedance calculations and the fault impedances on fault occurrence are, therefore, compared with these preset constant values by the relay which then initiates trips whenever lower impedances are detected. So, a distinction is made between the line impedance settings and the fault impedances. Similarly, for high impedance faults, the relays will not operate and clear as they do not pick up impedances higher than the line impedance and they would also fall out of the quadrilateral characteristics of the relay, especially in zone 1. This is usually the case during high resistance faults caused by, for example, fires and trees. These types of faults won't be detected especially in the zone 1 of the relay, but in some cases they may be detected in zone 2 or zone 3 which has some delayed operating times incorporated into the settings.

According to references [2]–[4] who did work on HV transmission lines, the compensation factor for the earth return (K_E) is defined as the ratio between the earth impedance and the impedance of the fault loop.

$$K_E = Z_E/Z_L \tag{8}$$

Hence, for a 2 × 25 kV AC autotransformer system which utilises a feeder and catenary;

$$Z_E = Z_r \tag{9}$$

$$Z_r = Z_{rail}//Z_{aew}//Z_{bec} \tag{10}$$

$$Z_L = Z_c//Z_f + Z_r \tag{11}$$

The impedance loop can be illustrated by Figure 9 and compensation factor for the earth return can, therefore, be defined as;

$$K_E = \left(\frac{Z_r}{Z_r + Z_c//Z_f}\right) \tag{12}$$

The results for this factor will also be discussed under Section VII.

VI. OHW LINE IMPEDANCE MEASUREMENTS SET-UP

In general, an OHW system consists of various components that can influence the line impedances, as well as factors like soil properties and adjacent conductors. These include the impedance parameters that were discussed in section IV. Therefore, to ensure the accuracy of distance protection calculations and settings, it is vital to obtain accurate OHW line impedances. On-site measurements eliminate the uncertainties and inaccuracies that may come with distance protection settings that are calculated using the manufacturer's conductor data.

The impedances were measured using a combination of the Omicron CPC 100 primary injection, variable frequency test and the Omicron CP CU1 coupling unit. Several test loops were set and current was injected into those loops and impedances were measured. Examples of the measurement circuits are given in Figures 9 and 10.

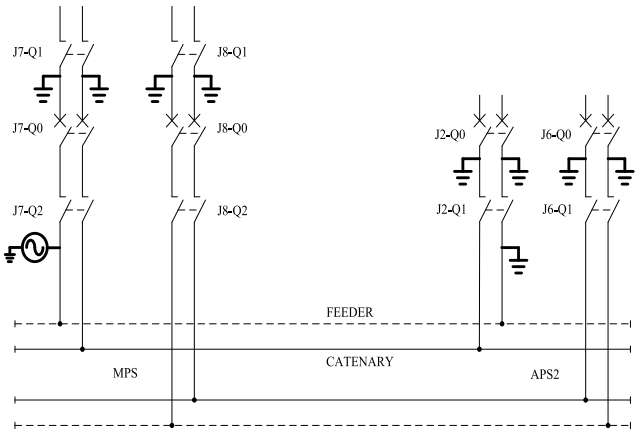

FIGURE 10. Feeder to earth measurements.

In the measurement set-up of Figures 9 and 10, some of the earth cables were installed for isolation purposes with some being installed to complete the measurement loop.

Using the setup in Figure 9, measurements were done between the MPS and APS2. A portable earth cable was installed at the APS and the variable test set was connected between the feeder and earth. A 50 A current was then injected at various frequencies varying from 30 Hz to 70 Hz and readings were recorded on the set. According to reference [3], [4] who conducted measurements on high voltage transmission lines, impedance measurements are more accurate when measured at the selected frequencies rather than the mains frequency. In Figure 10, measurements were done between the MPS and APS2. A portable cable was installed at the APS between the feeder and catenary in order to form a loop and the variable test set was connected between the feeder and catenary at the MPS. A 50 A current was then injected at 30 Hz and 70 Hz frequencies, and readings were recorded on the set. To confirm the accuracy of the results, a total of four measurements were conducted per each impedance loop.

TABLE 3. Track A catenary and feeder to earth measurements.

	Catenary to Earth Measurements			Feeder to Earth Measurements		
Frequency (Hz)	R (Ω)	X Ω)	Angle (...°)	R (Ω)	X (Ω)	Angle (...°)
30	1.945	5.786	71.42	2.240	7.949	74.26
30	1.945	5.785	71.41	2.239	7.950	74.27
70	2.050	5.667	70.11	2.363	7.779	73.11
70	2.049	5.667	70.12	2.359	7.781	73.13
Average	1.997	5.726	-	2.300	7.864	-

TABLE 4. Feeder to catenary measurements.

	Feeder to Catenary Measurements (Track A)			Feeder to Catenary Measurements (Track B)		
Frequency (Hz)	R (Ω)	X (Ω)	Angle (...°)	R (Ω)	X (Ω)	Angle (...°)
30	3.445	10.333	71.56	3.425	10.317	71.42
30	3.443	10.335	71.58	3.395	10.322	71.55
70	3.529	10.285	71.06	3.533	10.287	71.10
70	3.526	10.285	71.08	3.520	10.286	71.06
Average	3.486	10.309	-	3.47	10.30	-

TABLE 5. Measurements between Track A and Track B.

	Catenary (Track A) to Catenary (Track B) Measurements			Feeder (Track A) to Feeder (Track B) Measurements		
Frequency (Hz)	R (Ω)	X (Ω)	Angle (...°)	R (Ω)	X (Ω)	Angle (...°)
30	3.269	9.125	70.29	3.796	14.384	75.22
30	3.270	9.124	70.28	3.794	14.383	75.23
70	3.353	9.047	69.66	3.954	14.212	74.45
70	3.353	9.047	69.66	3.954	14.212	74.45
Average	3.311	9.086	-	3.874	14.298	-

As can be seen from the results in Tables 3 to 5, the difference between the maximum and minimum measured values is very small. The Omicron equipment measures with a degree of high accuracy.

VII. LINE IMPEDANCE MEASUREMENTS RESULTS AND COMPARISON WITH CALCULATED IMPEDANCES FROM DATA SHEETS

Although the Gautrain railway network comprises of six Substations including one MPS and five APSs, only the results between the MPS and APS2, and a summary of MPS to APS1 are discussed in this paper. The APSs are named APS1 to APS5. APS1 and APS2 are the nearest to the MPS, whereby, APS1 is located on the southern side of the neutral section shown in Figure 1, and APS2 is located on the northern side of the neutral section. APS3 is located north of APS2 and APS4 is located north of APS3 at the end of the tracks. APS5 is located near the OR Tambo airport, east of APS1 and close to the end of the tracks. APS1 is located at the beginning of a 16 km tunnel and there is no other APS south of APS1 at the end of track, hence, no impedance protection is applied in the tunnel section. For clarity on the results, the location of the APSs relative to the MPS and the line sections are as illustrated on Figure 11.

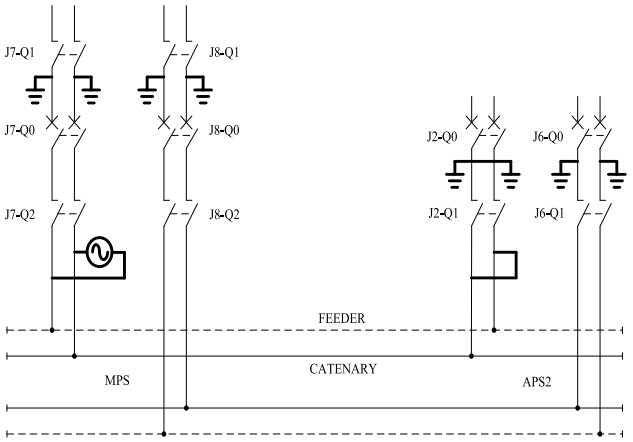

FIGURE 11. Catenary to feeder measurements.

In addition, the system comprises of two tracks, Track A and Track B, which run parallel to each other. Table 3 shows the impedances of Track A only, and Tables 4 and 5 are the impedances of both Track A and Track B.

Table 3 to 5 are the results of measurements conducted in two sections of the entire OHW system, namely MPS to APS2 and MPS to APS1, although the impedances of all line sections that are illustrated in Figure 11 were measured. Table 3 represents the catenary to earth impedance measurements, as well as, the feeder to earth impedance measurements for track A. The tables also show the impedance values at two different frequencies whose significance is explained section VI.

Tables 6 and 7 are the results summary showing the impedances that are used for protection settings calculations. The tables show a comparison between the new impedances obtained from the measurements and original impedance values calculated from the conductor data sheets. Table 6 shows the impedances of the line section from the MPS to APS2, whereas, Table 7 represents the impedances of the section of the traction line from the MPS to APS1.

NB: The % error is a comparison between measured values and the calculated impedance values.

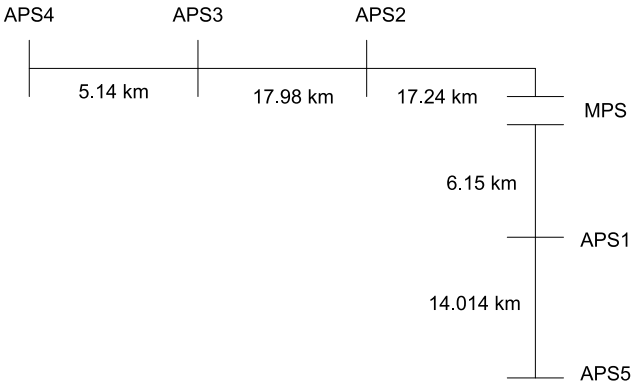

FIGURE 12. Location of all APS relative to the MPS.

TABLE 6. Results summary-MPS to APS2.

	Feeder		Catenary		Earth Return Circuit $R_{rail}//R_{BEC}//R_{AEC}$
	R (Ω)	X (Ω)	R (Ω)	X (Ω)	R (Ω)
New-Calculated from Measured Values	1.99	7.09	1.71	4.50	0.45
Original-Calculated from data sheet	2.10	3.06	3.28	2.22	0.41
% error	5.24	56.84	47.87	50.67	8.69

TABLE 7. Results summary-MPS to APS1.

	Feeder		Catenary		Earth Return Circuit $R_{rail}//R_{BEC}//R_{AEC}$
	R (Ω)	X (Ω)	R (Ω)	X (Ω)	R (Ω)
New-Calculated from Measured Values	0.71	2.53	0.61	1.61	0.164
Original-Calculated from data sheet	0.75	1.09	1.17	0.79	0.159
% error	4.00	56.92	47.86	50.93	3.14

Tables 8 and 9 are the earth return compensation factors for all the sections of the line. The tables are divided into north and south sections relative to the MPS and the neutral section.

Figures 12 and 13 are graphs comparing the measured impedances with the calculated impedances of the line section from the MPS to APS 2. Figures 14 and 15 are graphs comparing the measured impedances with the calculated impedances of the same line section from the MPS to APS1.

TABLE 8. Earth return compensation factor for north of line.

	MPS to APS2		APS2 to APS3		APS3 to APS4	
Z_r	0.41	1.64	0.41	1.45	0.16	0.55
Z_c	1.66	4.54	1.70	4.40	0.52	1.38
Z_f	1.94	7.15	2.01	7.04	0.58	1.68
$\lvert Z_c//Z_f \rvert$	2.93		2.87		0.81	
$\lvert Z_c//Z_f + Z_r \rvert$	4.62		4.37		1.38	
K_E	0.37		0.34		0.42	

TABLE 9. Earth return compensation factor for south of line.

	MPS to APS1		APS1 to APS5	
Z_r	0.16	0.68	0.44	1.32
Z_c	0.64	1.83	1.42	3.75
Z_f	0.73	2.56	1.72	5.92
$\lvert Z_c//Z_f \rvert$	1.12		2.43	
$\lvert Z_c//Z_f + Z_r \rvert$	1.82		3.82	
K_E	0.38		0.36	

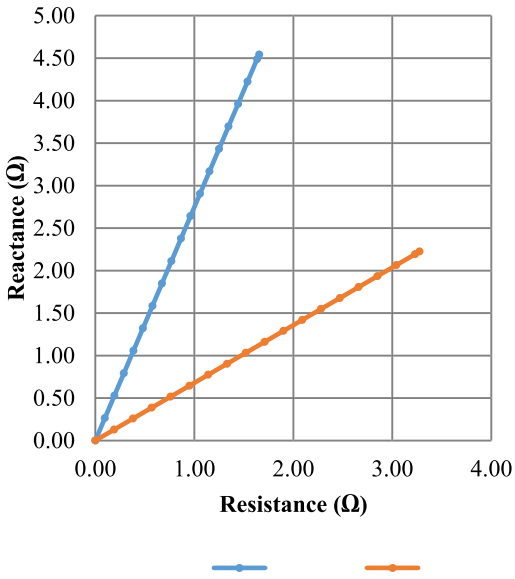

FIGURE 13. MPS to APS 2 Catenary Measured and Calculated Impedance Comparison.

VIII. DISCUSSIONS AND ANALYSIS OF RESULTS

The impedances of the catenary and feeder conductors differ because they are made of different conductor types with different parameters, and they also have different configurations.

In Table 3, for the catenary wire, the percentage difference between the resistance and reactance measured at 70 Hz and that measured at 30 Hz is 5.22 % and 2.06 % respectively. The percentage difference between the reactance measured

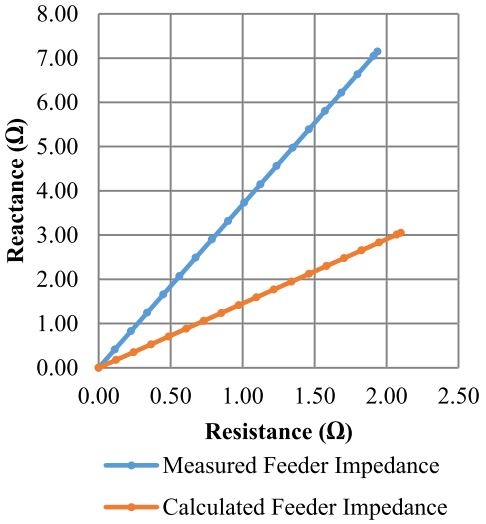

FIGURE 14. MPS to APS2 feeder measured and calculated impedance comparison.

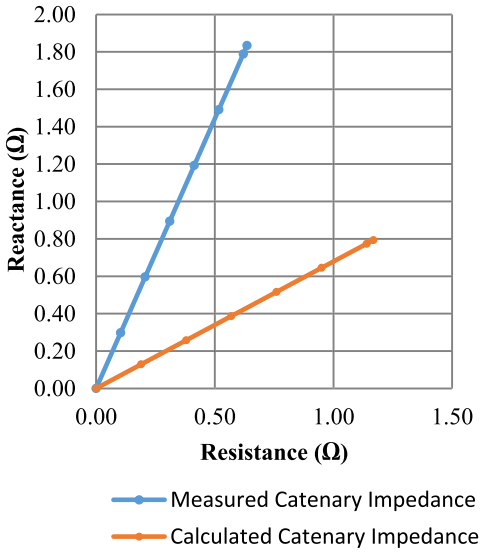

FIGURE 15. MPS to APS1 catenary measured and calculated impedance comparison.

at 70 Hz and that measured at 30 Hz is 2.06% and 2.14% for the catenary and feeder respectively.

In Table 3, for the feeder wire, the percentage difference between the resistance and reactance measured at 70 Hz and that measured at 30 Hz is 5.22% and 2.14% respectively. The protection settings are, therefore, based on the average impedance.

Table 4 represents the feeder to catenary measurements. In this table, the percentage difference between the impedance measured at 30 Hz and that measured at 70 Hz is smaller at 2.42% and 3.91% for the A and B line respectively. The percentage difference between the impedance measured at 30 Hz and that measured at 70 Hz is smaller at 0.49% and 0.35% for the A and B line respectively.

Table 5 represents impedance measurements between track A and track B. The catenary and feeder impedance were measured between track A and track B respectively. For these measurements, a portable cable was connected between the feeder conductors for both lines and between the catenary conductors for both lines at the APS and the current was injected at the MPS. As in the previous results, the percentage difference in impedance values is very small. The percentage difference between impedance at 30 Hz and impedance measured at 70 Hz for track A catenary to track B catenary measurements is 2.52% and 0.86% for the resistance and reactance respectively. Similarly, the percentage difference for the track A to track B feeder impedance is 4.06% and 1.20% for the resistance and reactance respectively.

Overall, the smaller percentage difference in the values measured shows that a change in the frequencies does not impact on the results. This is significant when making a decision to use measured impedances for settings calculations in that the frequencies other than 50Hz can be used without the need for any further validation for their accuracy. The protection settings are, therefore, based on the average impedance.

In Table 6 and Figure 14 for the catenary conductor impedances between MPS and APS2, there is an error of 47.87 % and 50.67 % for resistance and reactance respectively when comparing the calculated and the measure values. In Table 7 and Figure 14, for the catenary conductor, there is an error of 47.86 % and 50.93 % for resistance and reactance respectively.

In Table 6 and as illustrated in Figure 13, for the feeder conductor impedances between MPS and APS2, there is an error of 5.24 % and 56.84 % for the resistance and reactance respectively when comparing the calculated and the measured values. In Table 7 and figure 15, for feeder conductor, there is an error of 4 % and 56.92 % for the resistance and reactance respectively. This represents a significant percentage difference between the measured reactance and the original calculated values. The percentage error for the resistive component for the feeder wire is small at only 4 %.

Figure 16 shows a comparison between the measured and the calculated earth resistances for all line sections. The percentage error for the earth resistances varies from 3.14 % to 22.97 % in the line sections and it is independent of the section lengths. Therefore, the percentage error is independent of distance between the substations. From the graph, it is clear that earth measurements must be conducted per line section rather than using a single value for all sections.

Based on the results as discussed in this chapter, it is therefore, clear that there is value added in conducting impedance measurements for 2 × 25 kV AC traction systems. The percentage error between the impedance calculated from data sheets and the measured impedance is very significant and can result in over-reaching or under-reaching, thus, resulting in inaccurate and incorrect fault detection and operation of the relays.

The significant difference in the calculated impedance and the measured impedances can be attributed to the

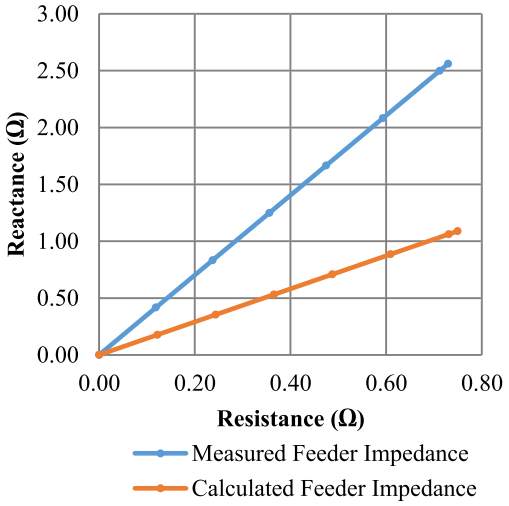

FIGURE 16. MPS to APS1 Feeder Measured and Calculated Impedance Comparison.

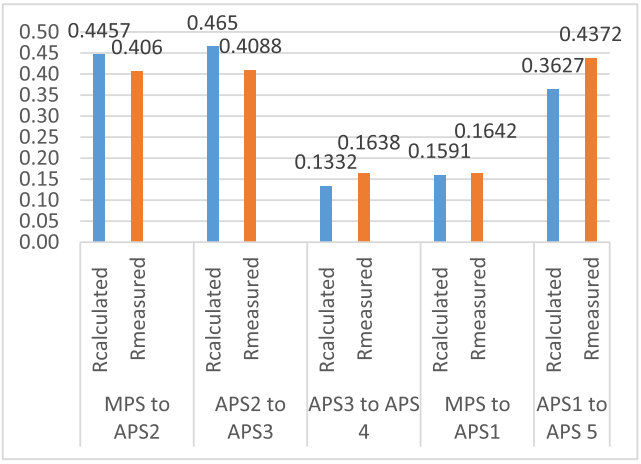

FIGURE 17. Measured and calculated earth resistance comparisons for all line sections illustrated in Figure 11.

OHW system configuration and the earth conditions that are described in section I of this paper. These include the soil resistivity, the line configuration, the feeder wire height, the contact wire height, earth wire height and the use of droppers relative to ground. In addition, a traction OHW system has constantly changing stagger and heights, for example, under the bridges, and cut and cover sections. The catenary system is expected to have a significant difference or error in calculated results as compared to the feeder because it is a combination of a contact wire and a catenary wire with several droppers along the entire network. It also contains a number of cross-overs and tension weights, whereas the feeder and earth wire are relatively straight conductors.

The earth return compensation factors are as shown in Tables 8 and 9, and on Figure 17. The results show that the line sections have different compensation factors. As can be seen in Figure 17, it is, therefore, important that when applying protection settings, this factor should be measured for each section and the settings should be based on this rather

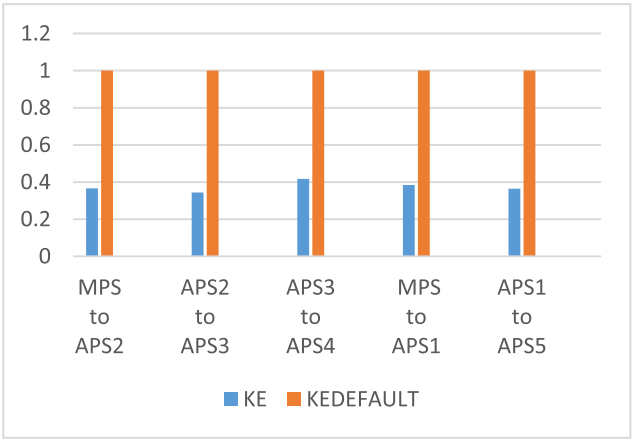

FIGURE 18. Comparison between the default setting and the measured compensation to earth circuit factor.

than default settings. Using a default setting and applying same settings in all sections can result in inaccurate protection settings.

IX. CONCLUSION

Without conducting line impedance measurements, the distance protection settings depend on the manual calculations and simulations using conductor data from the manufacturers. The conductor impedance per unit length is given by the manufacturers and total impedance is then calculated.

In this paper, the process of analysis and measurements of line and earth impedances was conducted in order to compare with theoretical or calculated values as given by the original equipment manufacturers of the conductors. As explained in the discussion and analysis of results, it is clear that measurements must be done as this process helps in improving the accuracy of impedance relay protection settings.

Measurements automatically take into consideration other factors influencing the impedances such as earthing grid, BEC, AEC, rail and other OHW components along the feeder and catenary. These measured impedances are used to recalculate protection settings to make them more accurate and reduce errors in relay operation. The earth return compensation factor K_E for each line section must the calculated from the measured impedances so that a correct protection setting can be applied.

Future Work: The overall results support the need for an impedance factor to be derived and included in future calculations to make the protection settings more accurate. The derived factor can only be used during design and implementation phase, however, once the system has been installed and the correct relays have been selected for the purpose, accurate measurements must be conducted and applied to the protection settings. Furthermore, an analysis can be done on the relation between the percentage error in catenary impedances to the total number of weights, and crossovers in a line section, and this can further be correlated to an impedance factor.

There is further opportunity in future work and through simulations, to show the influence of the autotransformers on fault impedances and how the measured fault impedances would relate to the distance to fault. Furthermore, there is an opportunity for future work on how the relationship between the calculated and measured impedances and their influence on the traction load and how far the impedances obtained by each one of the two methods would encroach on the traction load and the regenerative region in the characteristics of the relay used.

REFERENCES

[1] J. Izykowski, E. Rosolowski, and M. M. Saha, "Postfault analysis of operation of distance protective relays of power transmission lines," *IEEE Trans. Power Del.*, vol. 22, no. 1, pp. 74–81, 2007.

[2] L. Hulka, U. Klapper, M. Putter, and W. Wurzer, "Measurement of line impedance and mutual coupling of parallel lines to improve the protection system," in *Proc. 20th Int. Conf. Exhib. Electr. Distrib. (CIRED)*, Prague, Czech Republic, Jun. 2009, pp. 1–4.

[3] U. Klapper, M. Krüger, and S. Kaiser, "Reliability of transmission by means of line impedance and K-factor measurement," in *Proc. 18th Int. Conf. Electr. Distrib. (CIRED)*, Turin, Italy, Jun. 2005, pp. 1–4.

[4] A. Dierks, H. Troskie, and M. Krüger, "Accurate calculation and physical measurement of trasmission line parameters to improve impedance relay performance," in *Proc. IEEE Power Eng. Soc. Inaugural Conf. Expo. Afr.*, Durban, South Africa, Jul. 2005, pp. 455–461.

[5] L. Battistelli, M. Pagano, and D. Proto, "2 × 25-kV 50 Hz high-speed traction power system: Short-circuit modeling," *IEEE Trans. Power Del.*, vol. 26, no. 3, pp. 1459–1466, Jul. 2011.

[6] M.-K. Kim, M.-S. Kim, D.-H. Kim, and J.-W. Lee, "A study on the impedance calculation by using equivalent model in catenary system," *J. Railway*, vol. 3, no. 2, pp. 46–53, 2010.

[7] M. R. Ganjavi, R. Krebs, and H. Z. Styczynski, "Distance protection settings in electrical railway systems with positive and negative feeder," in *Proc. WSEAS Int. Conf. Energy Environ. Syst.*, Chalkida, Greece, 2006, pp. 357–361.

[8] N. Noroozi, H. Mokhtari, M. R. Zolghadri, M. Khodabandeh, A. Abazai, R. S. Khakshani, and S. Mazaheri, "Fault analysis on AC railway supply system," in *Proc. 6th Power Electron., Drive Syst. Technol. Conf. (PEDSTC)*, Tehran, Iran, Feb. 2015, pp. 567–572.

[9] Q. Li, "New generation traction power supply system and its key technologies for electrified railways," *J. Mod. Transp.*, vol. 23, no. 1, pp. 1–11, 2015.

[10] *Railway Applications—Supply Voltages of Traction Systems*, IEC Standard EN 50163, 2007.

[11] R. Skogberg, "Railway power supply system models for static calculations in a modular design implementation," M.S. Thesis, Dept. Elect. Eng., Royal Inst. Technol., Stockholm, Sweden, 2013.

[12] S.-H. Lee, J.-O. Kim, and H.-S. Jung, "Analysis of catenary voltage of an AT-fed AC HSR system," *IEEE Trans. Veh. Technol.*, vol. 53, no. 6, pp. 1856–1862, Nov. 2004.

[13] R. J. Hill and I. H. Cevik, "On-line simulation of voltage regulation in autotransformer-fed AC electric railroad traction networks," *IEEE Trans. Veh. Technol.*, vol. 42, no. 3, pp. 365–372, Aug. 1993.

[14] K. Wang, H. Hu, Z. Zheng, Z. He, and L. Chen, "Study on power factor behavior in high-speed railways considering train timetable," *IEEE Trans. Transport. Electrific.*, vol. 4, no. 1, pp. 220–231, Mar. 2018.

[15] R. D. White, "AC/DC railway electrification and protection," in *Proc. IET 13th Prof. Develop. Course Electr. Traction Syst.*, Nov. 2014, pp. 1–42.

[16] A. Dolara, M. Gualdoni, and S. Leva, "Impact of high-voltage primary supply lines in the 2 × 25 kV–50 Hz railway system on the equivalent impedance at pantograph terminals," *IEEE Trans. Power Del.*, vol. 27, no. 1, pp. 164–174, Jan. 2012.

[17] G. Varju, "Comparison of the booster transformer and auto transformer railway feeding systems, feeding features and induction to telecom lines," in *Proc. Electromagn. Compat. Conf. (EMC)*. York, U.K.: Univ. of York, Jul. 2004.

[18] E. Pilo, L. Rouco, A. Fernandez, and L. Abrahamsson, "A monovoltage equivalent model of Bi-voltage autotransformer-based electrical systems in railways," *IEEE Trans. Power Del.*, vol. 27, no. 2, pp. 699–708, Apr. 2012.

[19] T. Kulworawanichpong, "Optimising AC electric railway power flows with power electronic control," Ph.D. dissertation, Dept. Elect. Eng., Univ. Birmingham, Birmingham, U.K., 2004.

[20] C.-M. Lee, H.-S. Lee, D.-H. Yoon, H.-M. Lee, J.-Y. Song, G.-S. Jang, and B.-M. Han, "A novel fault location scheme on Korean electric railway system using the 9-conductor representation," *J. Elect. Eng. Technol.*, vol. 5, no. 2, pp. 220–227, 2010.

[21] A. Gopalakrishnan, M. Kezunovic, S. M. McKenna, and D. M. Hamai, "Fault location using the distributed parameter transmission line model," *IEEE Trans. Power Del.*, vol. 15, no. 4, pp. 1169–1174, Oct. 2000.

[22] E. Pilo, L. Rouco, A. Fernandez, and A. Hernández-Velilla, "A simulation tool for the design of the electrical supply system of high-speed railway lines," in *Proc. IEEE Power Eng. Soc. Summer Meeting*, Jul. 2000, vol. 2, pp. 1053–1058.

[23] M. Ceraolo, "Modeling and simulation of AC railway electric supply lines including ground return," *IEEE Trans. Transport. Electrific.*, vol. 4, no. 1, pp. 202–210, Mar. 2018.

[24] A. Mariscotti, P. Pozzobon, and M. Vanti, "Distribution of the traction return current in AT electric railway systems," *IEEE Trans. Power Del.*, vol. 20, no. 3, pp. 2119–2128, Jul. 2005.

[25] K.-H. Chao, P.-Y. Chen, and C.-H. Cheng, "Transient characteristics analysis based-on circuit models for a high-speed rail system," *WSEAS Trans. Circuits Syst.*, vol. 8, no. 11, pp. 853–862, 2009.

[26] H. S. Jung, S. H. Lee, and J.-O. Kim, "Analysis for autotransformer-fed AC electric railroad system using constant current mode with distribution-STATCOM," in *Proc. Mod. Electr. Power Syst. (MEPS)*, Wrocław, Poland, 2002, vol. 9, pp. 139–144.

NDAEDZO M. MOYO received the B.Sc. degree in electrical engineering and the M.Sc. degree in power and energy systems engineering from the University of KwaZulu-Natal, in 2000 and 2003, respectively, where he was specialized on HVDC Research. He is currently pursuing the Ph.D. degree in electrical engineering with the University of Pretoria. He was with the Electrical Transmission Division, Eskom, from 2003 to 2006. He has been with Bombela Maintenance (Pty) Ltd - a division of Bombardier Transportation, Gautrain Project, South Africa, since 2007. He specializes in HVDC and traction power supply systems. He has presented in eight conferences and published three journal articles, two of which are local journals.

RAMESH C. BANSAL (SM'03) has more than 25 years of diversified experience of research, scholarship of teaching and learning, accreditation, industrial, and academic leadership in several countries. He was employed by the University of Queensland, Australia, the University of the South Pacific, Fiji, BITS Pilani, India, and Civil Construction Wing, All India Radio. He was a Professor and the Group Head (Power) with the ECE Department, University of Pretoria (UP), South Africa. He has significant experience of collaborating with industry and Government organizations. He has made significant contribution to the development and delivery of the B.S. and M.E. degrees programmes for Utilities. He has extensive experience in the design and delivery of CPD programmes for professional engineers. He has carried out research and consultancy and attracted significant funding from Industry and Government Organizations. He is currently a Professor with the Department of Electrical and Computer Engineering, University of Sharjah. He has published more than 300 journal articles, presented articles at conferences, books, and chapters in books. He has Google citations of more than 7500 and h-index of 39. He has supervised 18 Ph.D. degree students, four Post Doctorates, and currently supervising seven Ph.D. degree students. His research interests include renewable energy (wind, PV, DG, and micro grid) and smart grid. He is a Fellow and Chartered Engineer IET-UK, a Fellow of Engineers Australia, a Fellow of the Institution of Engineers (India), and a Fellow of SAIEE. He is also an Editor of several highly regarded journals, IET-RPG, and the IEEE Systems Journals.

RAJ NAIDOO received the Ph.D. degree in electrical engineering from the University of Cape Town, South Africa, in 2008. He has more than 20 years of teaching, research, and industrial experience. He was the CEO and a Founder of Enermatics Energy and a Board Member of Stellenbosch Wind Energy Technologies. He has worked and consulted to several blue-chip companies. He is a currently the Director of EWYZE. He is also an Associate Professor with the Department of Electrical, Electronic, and Computer Engineering, University of Pretoria, South Africa. He has published many research articles in various journals and conferences. His research interests include the smart grid, renewable energy, and power systems.

WILLEM SPRONG gained valuable experience, while working for Transnet and Gibb (Pty) Ltd., in multidisciplinary railway engineering, including signalling, perway, civil, and electrical. As a registered Professional Electrical Engineer with 20 years of experience, he specializes in railway engineering and management environment, substations, reticulation, distributions, and transmission designs. He also specializes in the development and implementation of maintenance strategies, not limited to electrical engineering. He has also been involved in the development of strategies for training and safety management on different levels. Apart from his railway experience, he also has a wealth of experience in 6.6 and 11 kV distribution substations and overheads, 88-kV substation and system design, reticulation design, and indoor and indoor lighting design. His research interests include electrification design and project management, 3-kV direct current, 25, and 50 kV alternating current traction substation and overhead track equipment.

Dr. Sprong received various awards for his dedication to the engineering industry and community. These are CESA Young Engineer of the Year 2010 (Consulting Engineers South Africa), the 2010 Diamond Award for Outstanding Achievement (Diamandveld High School), and the 2012 Humanitarian Excellence Award (GIBB).